

7. YOUNG'S MODULUS AND VOIDAGE

When the large panel potential application of this material is considered, the most appropriate property would be the flexural modulus. This effectively measures the material's stiffness with respect to bending deformation. However, the bending modulus is of the same order of magnitude as the Young's modulus and follows the same trend. [36] The focus in this study will therefore be on the Young's modulus.

In Chapter 3 the following formulation variables were identified attributing to the properties of a composite:

- the shape and orientation of the reinforcing agent
- particle size and distribution
- concentration of polymer
- the degree of interfacial adhesion.

Each of these affect the composite in a different manner, as described earlier. The ANOVA results presented in the preceding sections revealed that:

- particle size contributed the most towards the Young's modulus (32%), with the wt% polymer second (16%). The contributions were, however, small compared to the error.
- the modification technique used contributed 11% towards the average performance, with even less significance than the other parameters tested.
If these are compared with the results for the flexural modulus, it is evident that the amount of polymer used is the most significant variable.
- concerning the preparation variables, pressure contributed the most towards the Young's modulus.

Compared with the results for the flexural modulus, it is evident that pressure is the most important preparation variable. Particle shape will ultimately influence the ability for good packing of particles in the composite. Bad packing will result in a

in a high voidage, especially when the percentage polymer is low. Using a high pressure during manufacture will help reduce the voidage caused by poor packing.

The ideal model to predict the Young's modulus of a systems should therefore:

- include the amount of binder resin (polymer)
- take into account the particle size or aspect ratio of the filler
- account for packing inefficiencies and mis-alignment of the filler
- make provisions for the adhesion efficiency between the filler and binder resin.

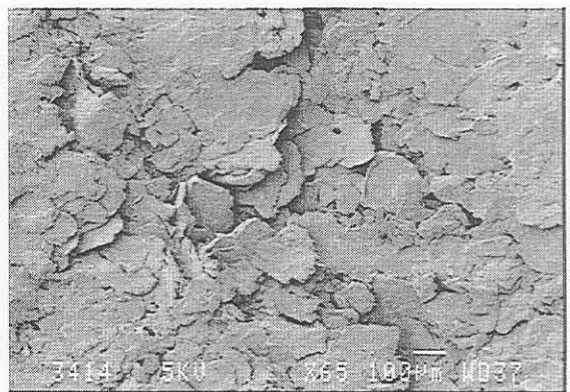
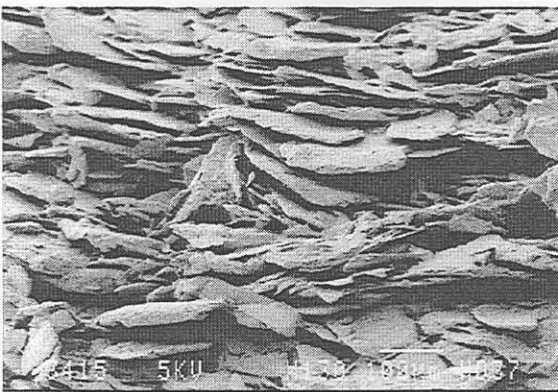
In the proposed model the following assumptions are made:

- the binder resin (LLDPE) and filler (phlogopite) are linear elastic
- the plates are rectangular and have uniform width and thickness.

Deviations from this assumption are accounted for by postulating a voidage for the composite. It is evident that when the volume fraction polymer is zero, the voidage is not zero.

- the plates are aligned in a plane parallel format

The compression moulding technique ensures proper alignment. Figure 14 shows the SEM photo of a composite comprising 8% LLDPE. Note that the binder was etched away to reveal the orientation.



A: Side view

B: Top view

Figure 14: Side and top view of a LLDPE / phlogopite composite, containing 8% LLDPE

- there is perfect bonding between the resin and the filler.

in a high voidage, especially when the percentage polymer is low. Using a high pressure during manufacture will help reduce the voidage caused by poor packing.

The ideal model to predict the Young's modulus of a systems should therefore:

- include the amount of binder resin (polymer)
- take into account the particle size or aspect ratio of the filler
- account for packing inefficiencies and mis-alignment of the filler
- make provisions for the adhesion efficiency between the filler and binder resin.

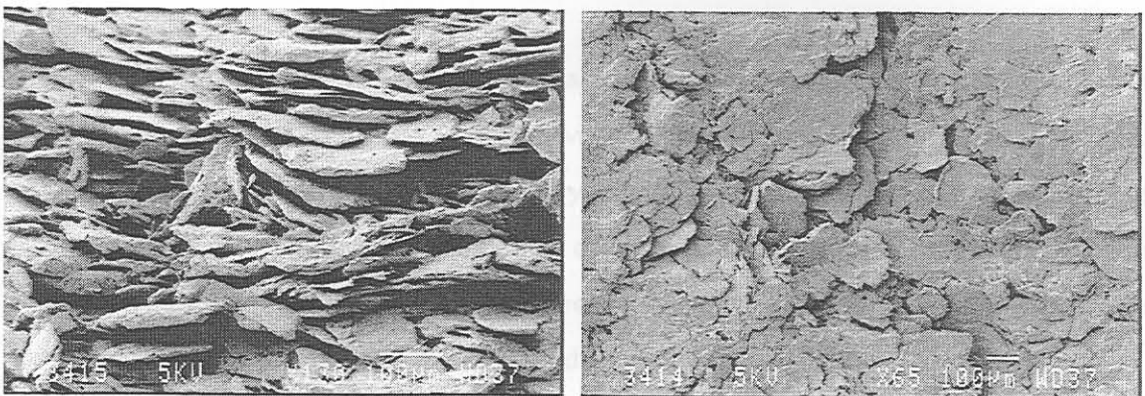
In the proposed model the following assumptions are made:

- the binder resin (LLDPE) and filler (phlogopite) are linear elastic
- the plates are rectangular and have uniform width and thickness.

Deviations from this assumption are accounted for by postulating a voidage for the composite. It is evident that when the volume fraction polymer is zero, the voidage is not zero.

- the plates are aligned in a plane parallel format

The compression moulding technique ensures proper alignment. Figure 14 shows the SEM photo of a composite comprising 8% LLDPE. Note that the binder was etched away to reveal the orientation.



A: Side view

B: Top view

Figure 14: Side and top view of a LLDPE / phlogopite composite, containing 8% LLDPE

- there is perfect bonding between the resin and the filler.

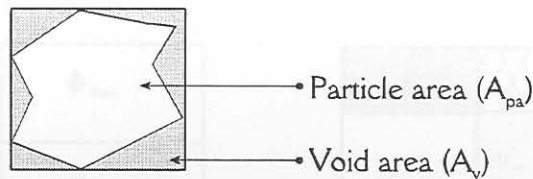
of the flakes. The maximum voidage is defined as the fraction free volume when this bed is densely compacted. It can be calculated using Equation 9.

$$\phi_m = 1 - \frac{V_{particle}}{V_{apparent}} \quad (9)$$

For the case of a single platelet with its associated void volume, it can be expressed in terms of projected surface areas:

$$\phi_m = \frac{A_v \times t}{(A_v + A_{pa}) \times t}$$

where t is the plate thickness.

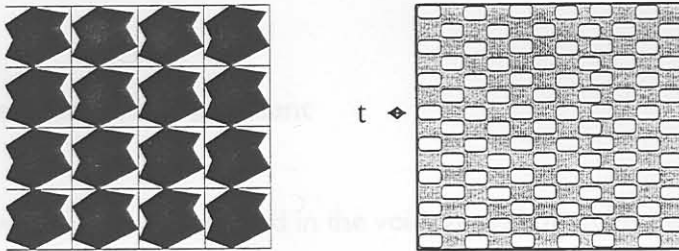


7.1.2 Total voidage

For a composite that contains matrix material there are two limiting situations. If the polymer during processing has a very low viscosity it will first fill the empty space available. If, however, the viscosity is very high, very little of the voidage will be filled. In practice the voidage of thermoplastic composites depends strongly on the temperature and the pressure applied during sheet manufacture. However, the two limiting situations define upper and lower bounds for the final voidage (See Figure 17).

The voidage, ϕ , of the composite can be calculated from the fraction open volume remaining after polymer has been added to aligned particles at maximum packing density. Consider a unit volume of such a composite as illustrated below. The voidage of such a composite could be modelled using the scheme proposed in Figure 16. It implies a specific

manner in which the resin partially displaces the reinforcement and fills the available void space.



- Particle volume fraction (V_f)
- Maximum voidage (ϕ_m)

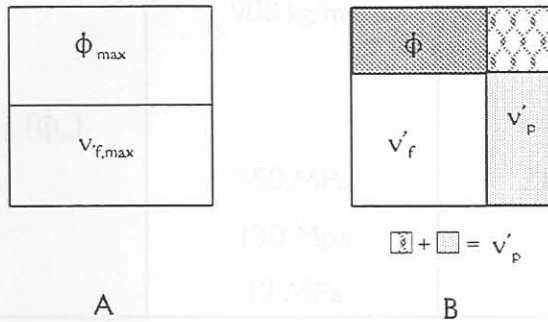


Figure 16: Schematic representation of the void volume in a composite

In this unit volume of composite that contains a volume fraction v_f of reinforcement, the associated voidage is equal to:

$$\frac{\phi_m}{1 - \phi_m} v_f \tag{10}$$

The sum of the volume fraction must equal unity, i.e.

$$\phi + v'_p + v'_f = 1 \tag{11}$$

Combining these two equations leads to a simple expression for voidage as a function of volume fraction polymer: (A more detailed discussion is presented in Appendix 2)

$$\phi = \frac{(1 - v_p')^2 \phi_m}{1 - v_p' \phi_m} \quad (12)$$

7.1.3 Correlation with experiment

Table 9 shows the parameters used in the voidage and modulus models.

Table 9: Parameter values used in models (Equation 12 and Equation 24)

	Polymer (LLDPE)	Phlogopite
Density	900 kg/m ³	3000 kg/m ³
Plate aspect ratio		18
Maximum packing (ϕ_m)		0.5
Young's modulus	350 MPa	21 GPa
Shear modulus	130 Mpa	
Shear strength	12 MPa	

7.2 Modelling the Young's modulus

Figure 17 shows that this model (Equation 12) provides a reasonable fit to the experimental data. It also suggests that the voidage does not depend on the particle size. This is not unexpected since it is known that the density of, for example, a randomly packed bed of spheres is independent of particle size. [37] The maximum packing density does, however, depend on the shape and orientation of the particles in the composite.

It is assumed that the average strain will be uniform when a force, F , is applied to the composite. Cox [38] proposed that the stress in the polymer layer is transferred to the

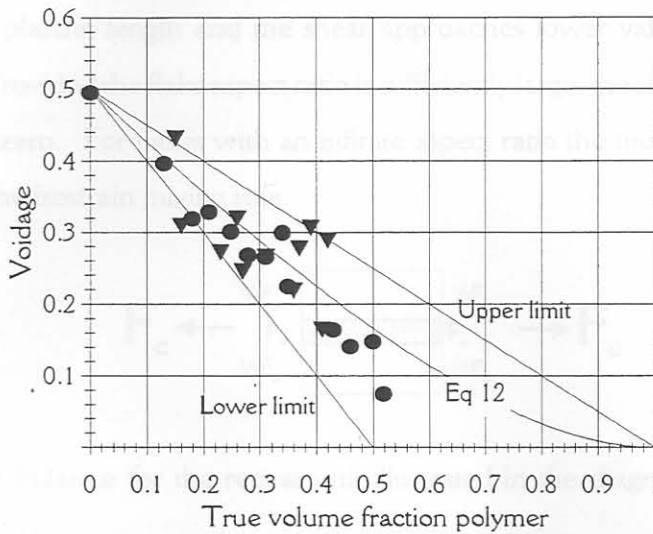
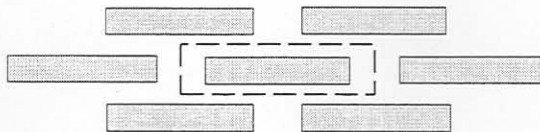


Figure 17: Composite voidage as a function of the volume fraction polymer (V_p). Particle size: \blacktriangledown : 250-300 μm \bullet : 125- 80 μm . $\phi_m = 0.5$

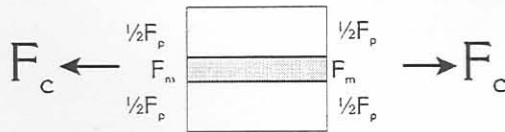
7.2 Modelling the Young's modulus

Consider a system where the reinforcements are rectangular platelets aligned parallel to the applied force. The dashed lines in the diagram below define a repeat unit that is representative of the composite.



It is assumed that the average strain will be uniform when a force, F , is applied to the composite. Cox [38] proposed that the stress in the polymer layer is transferred to the

flakes via a shear mechanism. Since the plates are discontinuous the shear force will be a maximum at the edges of the individual particles. Stress transfer occurs progressively along the platelet length and the shear approaches lower values at the middle of the platelet. Provided the flake aspect ratio is sufficiently large, the shear will actually decrease to almost zero. For flakes with an infinite aspect ratio the modulus of the composite is given by the isostrain mixing rule.



7.2.2 Shear in the polymer

The force balance for the repeat unit illustrated in the diagram above, is as given by Equation 13:

$$F_c = F_m + F_p \quad (13)$$

From the previous argument, stating that stress is transferred by a shearing mechanism, it follows that the total stress cannot be transferred between the polymer and the plates and the load carried by the plates will therefore be lower than predicted by the isostrain mixing rule.

7.2.1 Tensile force in the platelet

With the particles being discontinuous, the force acting on the platelet will be a function of the length of the particle. The nett result is that the displacement in the particle will also vary with length. Thus F_m , in Equation 13, describes the average force acting on the platelet.

The tensile stress in the platelet, as a function of distance from the edge of the platelet,

x , is described by Hooke's law as $\sigma_f(x) = \frac{du}{dx} E_m$. The corresponding force acting

on the platelet (with area $A_t = tW$) is therefore:

$$F_m(x) = E_m(tW) \frac{du}{dx} \quad (14)$$

7.2.2 Shear in the polymer

Perfect bonding between the two phases is assumed. Thus the displacement of the polymer layer is restrained by the platelet. The result is a shear force in the polymer which reaches a maximum at the edges of the platelet. The tensile force transmitted to the particle will therefore be a minimum at this point. Depending on the aspect ratio, a maximum value is reached at some distance along the platelet.

If the displacement of the polymer were v , at distance x , in the absence of the particle and the displacement of the particle is u (at distance x , from the edge), the displacement of the polymer will have been restrained by the distance ω . The shear force in the polymer therefore causes a shear strain γ , associated with the displacement, ω . Figure 18 illustrates the situation as described above.

The displacement due to the shear stress $d\tau$, is: $\omega = \frac{S}{2} \tan \gamma$, for small values of γ , ω

becomes: $\omega = \frac{S}{2} \gamma$. Hooke's law for shear deformation can be used to express the shear

deformation, i.e. the angle γ , as $\gamma = \frac{\tau}{G_p}$.

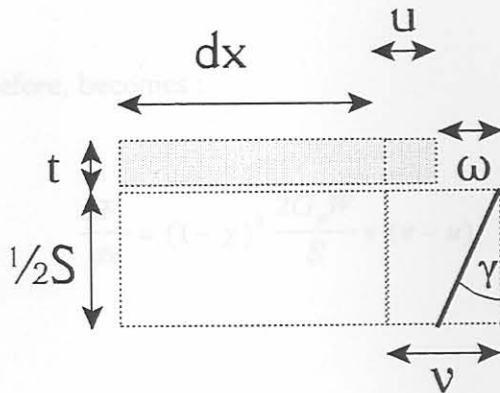


Figure 18: Shear strain in the polymer phase due to the restraining action of the platelet

The shear stress, τ , acts over the area dA_f , and the shear force is expressed as: $dF_s = \tau dA_f$, with $dA_f = W dx$

With $\omega = v - u$, the shear force can now be expressed as:

$$\frac{dF_s}{dx} = \frac{2G_p W}{S} (v - u) \quad (15)$$

The stress transfer will also be influenced by the voidage in the polymer phase, χ . The voidage will influence the area over which the shear force acts and is therefore $dx(1-\chi)$. The spacing between the plates is proportional to the volume fraction polymer and the true distance is therefore $\frac{S}{(1-\chi)}$, taking the voidage into account. The shear modulus

of the polymer will also be reduced by the factor $(1-\chi)$. The voidage in the polymer

phase can be calculated relative to the composite voidage, ϕ , as $\chi = \frac{\phi}{v_p(1-\phi) + \phi}$.

Equation 15, therefore, becomes :

$$\frac{dF_s}{dx} = (1-\chi)^3 \frac{2G_p W}{S} \times (v-u) \quad (16)$$

7.2.3 Average tensile force in the particle

Equations 14 and 16 can be combined by noting that $2dF_s = -dF_m$ and that $\frac{dv}{dx} = \varepsilon$,

where the strain, ε , in the polymer, in the absence of the platelet, is constant. The result is:

$$\frac{dF_m^2}{dx} = \frac{(1-\chi)^3 4G_p W}{S} \times \left(\frac{F_m}{E_m t W} - \varepsilon \right) \quad (17)$$

Equation 17 can be solved by using the Laplace transformations, with boundary conditions are $F_m = 0$ when $x = 0$ and $F_m = 0$ when $x = D$. After some mathematical manipulation the result is (See Appendix 2):

$$F_m(x) = E_m t W \varepsilon \left(1 - \frac{\cosh(\mu \frac{D}{2} - \mu x)}{\cosh(\mu \frac{D}{2})} \right) \quad (18)$$

where :

$$\mu = \sqrt{\frac{(1-\chi)^3 4G_p}{SE_m t}}$$

The average force F_m can be found by integrating Equation 18 over the length D and dividing by the total length D . The result is:

$$F_m = E_m t W \varepsilon \left(1 - \frac{\tanh(\varphi)}{\varphi} \right) \quad (19)$$

where:

$$\varphi = \sqrt{\frac{(1 - \chi)^3 G_p D^2}{S E_m t}} \quad (20)$$

The aspect ratio of the flakes is given by $\alpha = \frac{D}{t}$. The ratio $\frac{t}{S}$ can be expressed in terms of volume fractions. This reduces Equation 20 to:

$$\varphi = \alpha \sqrt{\frac{(1 - \chi)^3 G_p}{E_m} \times \frac{v_f}{1 - v_f}} \quad (21)$$

7.2.4 Composite modulus

7.2.5 Comparison with experiment

For the composite Equation 13 can be expressed as:

$$\frac{F_c}{A_c} A_c = F_m + \frac{F_p}{A_p} A_p \quad (22)$$

The area occupied by the plates is: $A_m = t \times W$ and the area of the polymer is: $A_p = s \times W$, where W is the width of the plates. The total area over which force F_c is applied is: $A_c = (s + t)W$. Equation 22 can therefore be written as:

$$\sigma_c = \frac{F_m}{(S + t)W} + \frac{S}{(S + t)} \sigma_p \quad (23)$$

With F_m given by Equation 19 and the ratios $\frac{t}{s+t}$ and $\frac{s}{s+t}$ the volume fraction platelets, v_f and polymer, v_p respectively. Noting that the Young's modulus of an elastic material is given as $E = \frac{\sigma}{\epsilon}$ and assuming that the composite is under a uniform strain, ϵ ,

Equation 23 can be reduced to:

$$E_c = v_f E_m MRF + v_p E_p \quad (24)$$

where the modulus reduction factor (MRF) is given by:

$$MRF = \left(1 - \frac{\tanh(\phi)}{\phi} \right) \quad (25)$$

The result is similar to that of Cox [38] as modified by Padawer and Beecher [27], apart from the correction for voidage. This correction is critical as it provides the correct limit of zero modulus for a particulate composite in the absence of matrix. Figure 19 graphically compares the modulus correction factors.

7.2.5 Comparison with experiment

Figure 20 shows the results obtained for the Young's modulus of the composites, as described in Section 5.4, and the predicted Young's modulus, calculated using Equation 24 together with Equation 12 for voidage. The predicted modulus values are very close to the experimentally measured ones. This confirms that the present model overcomes the drawbacks of previous models for the case where the matrix is present in very low concentrations. Figure 21 compares the new model with previous ones. It predicts much lower values for the Young's modulus. For high volume fraction polymer its predictions are similar to those of the model by Padawer and Beecher [27] and the isostrain mixing rule.

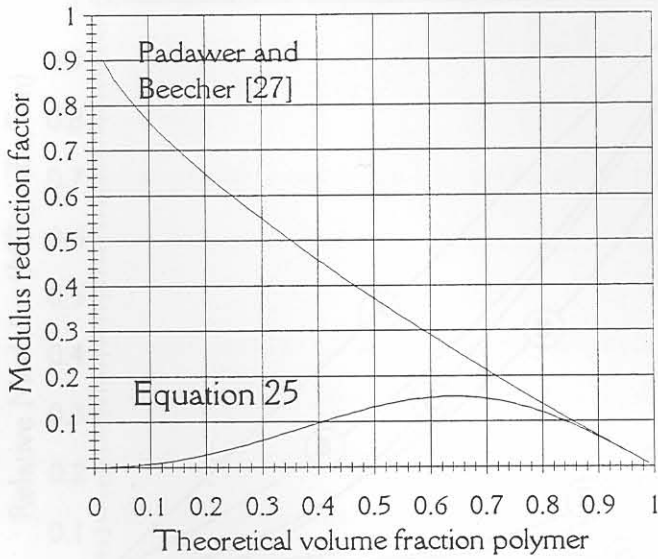


Figure 19: Comparison of the modulus reduction factors of Cox[38], as modified by Padawer and Beecher [27] with Equation 25 together with Equation 12

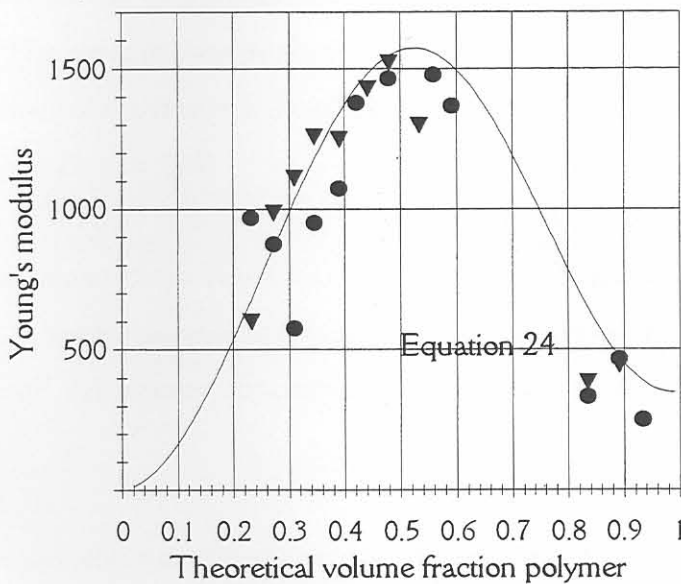


Figure 20: Measured modulus (● 125 - 180 μm) and the modulus calculated with Equation 24. Parameter values are given in Table 9

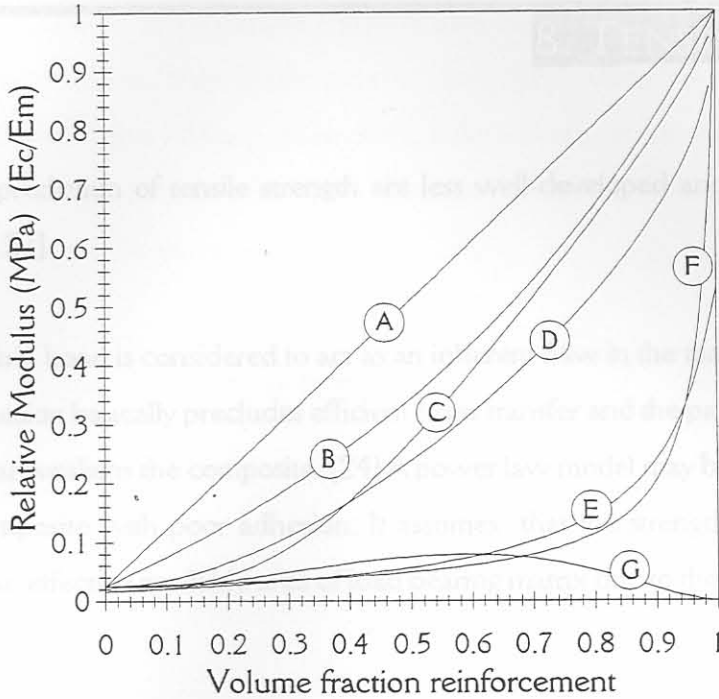


Figure 21: The predicted variations of the tensile modulus of a composite: A: Isostrain (1A), B: Jacquet et al. (4), C: Padawer and Beecher (5A), D: Luis et al. (5B), E: Kerner and Lewis (6), F: Isostress (1B), G: Equation 24. Quantities in brackets indicate the equation numbers in the main text.